JCAMECH
Vol. 46, No. 2, July 2015, pp 93- 105

Vibration analysis of double bonded composite pipe reinforced by BNNTs conveying oil

A. Ghorbanpour Arani[1,2*], E. Haghparast[2] and Z. Khoddami Maraghi[2]

1. Institute of Nanoscience & Nanotechnology, University of Kashan, Iran

2. Department of Mechanical Engineering, University of Kashan, Iran

Received 7 October 2014; Accepted 7 May 2015

Abstract

In the present research, nonlinear vibration in a coupled system of Boron-Nitride nano-tube reinforced composite (BNNTRC) oil pipes is studied. Single-walled Boron-Nitride nano-tubes (SWBNNTs) are arranged in a longitudinal direction inside Poly-vinylidene fluoride (PVDF) matrix. Damping and shearing effects of surrounded medium are taken into account by visco-Pasternak model. Based on piezoelectric fiber reinforced composite (PFRC) theory, properties of smart coupled BNNTRC oil pipes are obtained. The equations of motion as well as the boundary conditions are derived using Hamilton's principle. The effects of various parameters such as volume fraction and orientation angle of fibers, viscosity and density of fluid on stability of coupled BNNTRC oil pipes are investigated. Results indicate that stability of smart composite system is strongly dependent on angle orientation and volume percent of BNNTs. Results of this investigation can be used in oil refineries.

Keywords: *Coupled oil pipes, Polymeric nano-composite, Visco-elastic foundation, PFRC theory.*

1. Introduction

In the past several years, many researchers have focused on nano-tube reinforced composite properties and discovered that mechanical, electrical and thermal properties of polymer composites can be significantly improved when small percent of nano-tube such as carbon nano-tubes (CNTs) and BNNTs add as fibers. Although, the main purpose of these investigations are development of this advanced material in actual structures. Premium features of nano-tubes (high strength and stiffness) causes to utilize it as reinforcement instead of conventional fibers in nano/ micro-composite structures such as beam, plate and shell. Introduction of BNNT as a piezoelectric material which have coupled the electro-mechanical effects into polymer matrix, upgrade the application of nano/ micro-composites and make a system of smart materials.

In recent years, various researches have been carried out to analyze buckling, dynamic stability, and free vibration of the smart structures in which the shell theory have been

* Corresponding Author Email: aghorban@kashanu.ac.ir

employed. Using generalized differential quadrature method (GDQM), Shu [1] investigated free vibration of composite conical shell reinforced with a piezoelectric layer. Free vibration and buckling analysis of composite cylindrical shells conveying hot fluid was studied by Kadoli and Ganesan [2].

The axisymmetric temperature variation and the steady flow of hot fluid in the composite shell were assumed in their study. They utilized first order shear deformation theory to model the elastic shells. Their results demonstrated that the influence of fiber angle on the critical mean axial velocities is considerable.

A three-dimensional solution of smart laminated anisotropic circular cylindrical shells with imperfect bonding was presented by Wang and Zhang [3]. Salehi-Khojin and Jalili [4] studied the buckling behaviour of BNNT reinforced PVDF under combined electro-thermo-mechanical loadings. They used Donnell shell theory to obtain governing equations of motion. In addition, they developed a new equivalent spring constant model of piezoelectric matrix under electro-thermo-mechanical loadings based on Whitney–Riley model. Their results showed that applying direct and reverse voltages to BNNT changes the buckling loads for any axial and circumferential wave numbers.

Amabili et al. [5] researched fluid filed, conveying fluid and empty tubes as a circular cylindrical shell. Both Donnell and Sanders–Koiter nonlinear theories were used to obtain stain-displacement relations of the shell. The fluid was modelled by potential flow theory but the effect of steady viscous forces was taken into account. They used Non-classical boundary conditions to simulate the conditions of experimental tests in a water tunnel. In addition, the comparison between numerical and experimental results was performed in their study. Free vibration response of composite sandwich cylindrical shell with flexible core was studied by Rahmani et al. [6]. Their results revealed that the sandwich shells with flexible core exhibit a complex behaviour and the vibration patterns of the sandwich cylindrical shells are more complex than those of the homogeneous shells. Furthermore, it was observed that the natural modes of the sandwich shell are different from those of the sandwich plate and have a mixed mode nature.

Vibration and stability of micro-scale cylindrical shell conveying fluid was conducted by Zhou and Wang [7]. They employed modified couple stress theory to consider size effect. Governing equations are obtained by means of classical shell theory.

It was concluded that larger size effect of the natural frequencies is shown for smaller-size micro-scale shell containing static fluid, and much larger size effect is shown for the micro-scale shells conveying fluid with a certain flow velocity, as compared with that of the empty shell.

Based on nonlocal piezo-electricity theory, vibration and buckling behaviour of double-walled Boron-Nitride nano-tubes (DWBNNTs) embedded in an elastic medium with and without fluid was studied by Ghorbanpour Arani et al. [8-9]. They showed that the electric field effect on the frequency is approximately constant, while it decreases with increasing temperature change. Also, they concluded that the electric field and its direction have affected the magnitude of the critical buckling load. In the other work, Ghorbanpour Arani et al. [10] researched into the nonlinear nonlocal vibration and instability of conveyed micro-tube reinforced by BNNT using Donnell's shell theory. Their results showed that increasing volume fraction and angle orientation of fiber causes to increase stiffness of micro-tube.

Based on modified couple stress theory, Ghorbanpour Arani et al. [11] studied on nonlinear vibration of embedded smart composite microtube conveying fluid. They used Timoshenko beam (TB) model to obtain governing equations of motion. They demonstrated that the material properties of matrix and reinforcement have a significant role on stability of microtube.

However, vibration analysis of coupled system of BNNTRC oil pipes conveying viscous fluid embedded in an elastic medium is a novel topic that it hasn't been found in literature. Motivated by these considerations, our aim is to study of electro-thermal vibration analysis of coupled composite oil pipes which is placed in uniform temperature and electric fields. Oil pipes are simulated by cylindrical shell model and they have been coupled together with visco-Pasternak medium. Higher-order equations of motion have been derived based on Hamilton's principle and differential quadrature method (DQM) is applied to obtain

vibrational response of coupled composite system. Results of this investigation can be used in oil refineries.

2. Constitutive equations based on PEFRC theory

To obtain properties of coupled composite oil pipes, a representative volume element (RVE) has been considered and micro-mechanical method known as "XY PEFRC" or "YX PEFRC" [12-13] is employed. In this modelling, both matrix and reinforcement are assumed to be smart and the BNNTs are considered as a longitudinal straight fibers in both oil pipes. According to the XYPEFRC micro-mechanical method, the constitutive equations for the electro-thermo-mechanical behavior of the selected RVE are expressed as [10]:

$$\begin{Bmatrix}\sigma_1\\ \sigma_2\\ \sigma_3\\ \tau_{23}\\ \tau_{31}\\ \tau_{12}\\ D_1\\ D_2\\ D_3\end{Bmatrix}=\begin{bmatrix}C_{11} & C_{12} & C_{13} & 0 & 0 & 0 & 0 & 0 & -e_{31}\\ C_{12} & C_{22} & C_{23} & 0 & 0 & 0 & 0 & 0 & -e_{32}\\ C_{13} & C_{23} & C_{33} & 0 & 0 & 0 & 0 & 0 & -e_{33}\\ 0 & 0 & 0 & C_{44} & 0 & 0 & 0 & -e_{24} & 0\\ 0 & 0 & 0 & 0 & C_{55} & 0 & -e_{15} & 0 & 0\\ 0 & 0 & 0 & 0 & 0 & C_{66} & 0 & 0 & 0\\ 0 & 0 & 0 & 0 & e_{15} & 0 & \in_{11} & 0 & 0\\ 0 & 0 & 0 & e_{24} & 0 & 0 & 0 & \in_{22} & 0\\ e_{31} & e_{32} & e_{33} & 0 & 0 & 0 & 0 & 0 & \in_{33}\end{bmatrix}\begin{Bmatrix}\varepsilon_1\\ \varepsilon_2\\ \varepsilon_3\\ \gamma_{23}\\ \gamma_{31}\\ \gamma_{12}\\ E_1\\ E_2\\ E_3\end{Bmatrix}-\begin{Bmatrix}\lambda_1\\ \lambda_2\\ \lambda_3\\ \lambda_4\\ \lambda_5\\ \lambda_6\\ p_1\\ p_2\\ p_3\end{Bmatrix}\Delta T, \tag{1}$$

where $\{\sigma_i\},\{\tau_{ij}\}$, $\{\varepsilon\},\{\gamma_{ij}\}$, $\{D\}$ and $\{E\}$ are normal stresses, shear stresses, normal strains, shear strains, electric displacement and electric field vectors, respectively. Also, $[C]$, $[e]$ and $[\in]$ are matrices of elastic stiffness, piezoelectric and dielectric parameters, respectively. Furthermore, the coefficients of thermal expansion and pyroelectric are shown by $\{\lambda\}$ and $\{p\}$, respectively, and the temperature change is represented by ΔT. Assuming plane stress condition and unidirectional electric field along the pipe, equation (1) can be simplified as follows [7]:

$$\begin{Bmatrix}\sigma_{xx}\\ \sigma_{\theta\theta}\\ \tau_{x\theta}\\ D_x\end{Bmatrix}=[Q]\begin{Bmatrix}\varepsilon_{xx}\\ \varepsilon_{\theta\theta}\\ \gamma_{x\theta}\\ E_x\end{Bmatrix}-\begin{Bmatrix}\lambda_{xx}\\ \lambda_{\theta\theta}\\ \lambda_{x\theta}\\ p_x\end{Bmatrix}\Delta T, \tag{2}$$

where x and θ are longitudinal and circumferential coordinates with the origin located at the mid-plane of the oil pipes and matrix $[Q]$ is defined as:

$$[Q]=\begin{bmatrix}C_{xxxx} & C_{xx\theta\theta} & 0 & -e_{xxx}\\ C_{xx\theta\theta} & C_{\theta\theta\theta\theta} & 0 & -e_{x\theta\theta}\\ 0 & 0 & C_{x\theta x\theta} & 0\\ e_{xxx} & e_{x\theta\theta} & 0 & \in_x\end{bmatrix}. \tag{3}$$

The longitudinal component of electric field in terms of electric potential is defined as [7]:

$$E_x=-\frac{\partial\varphi}{\partial x}, \tag{4}$$

where ϕ denotes the scalar function of electric potential. To consider the effects of orientation angle of the BNNTs with respect to the longitudinal axis, the following transformation matrix can be employed as:

$$[\tilde{Q}]=[T][Q][T]^T. \tag{5}$$

The transformation matrix [T] is [14]:

$$[T]=\begin{bmatrix}\cos^2\alpha & \sin^2\alpha & 2\sin\alpha\cos\alpha & 0\\ \sin^2\alpha & \cos^2\alpha & 2\sin\alpha\cos\alpha & 0\\ -\sin\alpha\cos\alpha & \sin\alpha\cos\alpha & \cos^2\alpha-\sin^2\alpha & 0\\ 0 & 0 & 0 & 1\end{bmatrix}, \tag{6}$$

where α is the angle of BNNTs with respect to the pipes axis.

3. Donnel's shell theory

Figure 1 demonstrates two composite oil pipes which are coupled with visco-Pasternak medium. PVDF and BNNTs are selected as a matrix and reinforcement, respectively. Both oil pipes are conveying viscose fluid and nonlinear vibration of coupled smart system is investigated using shell theory.

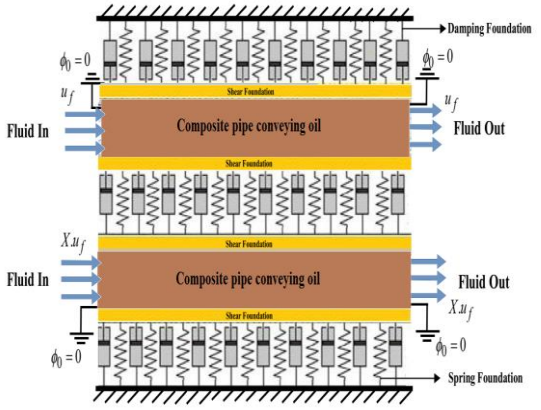

Fig. 1. Schematic of the coupled composite BNNTRC oil pipes embedded in visco-Pasternak medium

The displacement components of cylindrical shell in the axial (x), circumferential (θ), and radial (z) directions can be written as [15]:

$$\begin{aligned}
&\widetilde{U}_i(x,\theta,z,t) = u_i(x,\theta,t) - z\frac{\partial w_i(x,\theta,t)}{\partial x},\\
&\widetilde{V}_i(x,\theta,z,t) = v_i(x,\theta,t) - z\frac{1}{R_i}\frac{\partial w_i(x,\theta,t)}{\partial \theta},\\
&\widetilde{W}_i(x,\theta,z,t) = w_i(x,\theta,t),
\end{aligned} \tag{7}$$

where u_i, v_i and w_i refer to the displacement components of the middle surface of the shell in the axial, circumferential and radial directions, respectively. Also, z is the distance from an arbitrary point to the middle surface. Note that R_i is the mean radius of composite oil pipes. Here, $i = 1,2$ represent the upper and lower oil pipes, respectively. Based on Donnell's shell theory and applying equation (7), strain-displacement relationships may be written as [15]:

$$\begin{aligned}
&\varepsilon_{xxi} = \frac{\partial u_i}{\partial x} + \frac{1}{2}\left(\frac{\partial w_i}{\partial x}\right)^2 - z\frac{\partial^2 w_i}{\partial x^2},\\
&\varepsilon_{\theta\theta i} = \frac{1}{R_i}\frac{\partial v_i}{\partial \theta} + \frac{w_i}{R_i} + \frac{1}{2R_i^2}\left(\frac{\partial w_i}{\partial \theta}\right)^2 - \frac{z}{R_i^2}\frac{\partial^2 w_i}{\partial \theta^2},\\
&\varepsilon_{x\theta i} = \frac{1}{2R_i}\frac{\partial u_i}{\partial \theta} + \frac{1}{2}\frac{\partial v_i}{\partial x} + \frac{1}{2R_i}\frac{\partial w_i}{\partial \theta}\frac{\partial w_i}{\partial x} - \frac{z}{R_i}\frac{\partial^2 w_i}{\partial x \partial \theta}.
\end{aligned} \tag{8}$$

4. Strain energy

Based on shell theory, the strain energy of oil pipes is expressed as:

$$U_i = \frac{1}{2}\int_0^{2\pi}\int_0^{L}\int_{-h_i/2}^{h_i/2} (\sigma_{xx}\varepsilon_{xx} + \sigma_{\theta\theta}\varepsilon_{\theta\theta} + 2\tau_{x\theta}\varepsilon_{x\theta})\, dz dx R_i d\theta, \tag{9}$$

where $\sigma_{xx}, \sigma_{\theta\theta}$ and $\tau_{x\theta}$ are axial, circumferential and shear stresses, respectively.

5. Kinetic Energy

Velocity field vector ($\vec{V} = (V_x, V_\theta, V_z)$) for the fluid conveying through the composite oil pipes is the relative velocity of fluid and oil pipes which can be expressed as [15]:

$$\begin{aligned}
&V_{1x} = \frac{\partial \tilde{U}_1}{\partial t} + u_f\cos\theta_1, \qquad V_{2x} = \frac{\partial \tilde{U}_2}{\partial t} + X.u_f\cos\theta_2,\\
&V_{1z} = \frac{\partial \tilde{W}_1}{\partial t} - u_f\sin\theta_1, \qquad V_{2z} = \frac{\partial \tilde{W}_2}{\partial t} - X.u_f\sin\theta_2,\\
&V_{1\theta} = \frac{\partial \tilde{V}_1}{\partial t}, \qquad V_{2\theta} = \frac{\partial \tilde{V}_2}{\partial t}.
\end{aligned} \tag{10}$$

where $\theta_i = -\frac{\partial w_i}{\partial x_i}$ and u_f is the constant velocity of fluid and X is the ratio of fluid velocity in lower pipe than upper one.

According to Equation (11), the kinetic energy of coupled composite oil pipes and the kinetic energy associated with the fluid flow are, respectively, given by [15]:

$$\begin{aligned}
K_{pipes} = \frac{1}{2}\rho_t\int_0^{L}\Bigg[&\int_{A_1}\left[\left(\frac{\partial u_1}{\partial t} - z_1\frac{\partial^2 w_1}{\partial x \partial t}\right)^2 + \left(\frac{\partial v_1}{\partial t} - \frac{z_1}{R_1}\frac{\partial^2 w_1}{\partial \theta \partial t}\right)^2 + \left(\frac{\partial w_1}{\partial t}\right)^2\right] dA_1\\
&+ \int_{A_2}\left[\left(\frac{\partial u_2}{\partial t} - z_2\frac{\partial^2 w_2}{\partial x \partial t}\right)^2 + \left(\frac{\partial v_2}{\partial t} - \frac{z_2}{R_2}\frac{\partial^2 w_2}{\partial \theta \partial t}\right)^2 + \left(\frac{\partial w_2}{\partial t}\right)^2\right] dA_2\Bigg] dx,
\end{aligned} \tag{11}$$

$$\begin{aligned}
K_{fluid} = &\frac{1}{2}\rho_f\int_0^{L}\iint_{A_{1f}}\left\{\left(\frac{\partial \tilde{U}_1}{\partial t} + u_f\cos\theta_1\right)^2 + \left(\frac{\partial \tilde{W}_1}{\partial t} - u_f\sin\theta_1\right)^2 + \left(\frac{\partial \tilde{V}_1}{\partial t}\right)\right\} dA_{1f}\, dx\\
&+ \frac{1}{2}\rho_f\int_0^{L}\iint_{A_{2f}}\left\{\left(\frac{\partial \tilde{U}_2}{\partial t} + X.u_f\cos\theta_2\right)^2 + \left(\frac{\partial \tilde{W}_2}{\partial t} - X.u_f\sin\theta_2\right)^2 + \left(\frac{\partial \tilde{V}_2}{\partial t}\right)\right\} dA_{2f}\, dx.
\end{aligned} \tag{12}$$

To evaluate the viscosity effect on the frequencies of coupled microtubes, Navier-stokes equation can be used as follows [16, 17]:

$$\rho_f\frac{d\vec{V}}{dt} = -\nabla P + \mu\nabla^2\vec{V}. \tag{13}$$

Substituting the fluid velocity in Equation (13) and applying surface integrals $\left(m = \int_A \rho\, dA\right)$ to Equation (13) viscosity terms were derived and added to the equations of motion.

6. External work

The forces due to surrounding elastic medium which is simulated by visco-Pasternak model are expressed as follows [18-21]:

$$\begin{aligned} F_1 &= -K_w w_1 + K_G \frac{\partial^2 w_1}{\partial x^2} - C_d \frac{\partial w_1}{\partial t} + K_w (w_2 - w_1) \\ &- K_G \frac{\partial^2 (w_2 - w_1)}{\partial x^2} + C_d \frac{\partial (w_2 - w_1)}{\partial t}, \\ F_2 &= -K_w w_2 + K_G \frac{\partial^2 w_2}{\partial x^2} - C_d \frac{\partial w_2}{\partial t} + K_w (w_1 - w_2) \\ &- K_G \frac{\partial^2 (w_1 - w_2)}{\partial x^2} + C_d \frac{\partial (w_1 - w_2)}{\partial t}. \end{aligned} \quad (14)$$

where F_1 is the external forces applied on upper pipe and F_2 is applied force on lower pipe. k_w, k_G and C_d are spring, shear and damping modulus, respectively. The external work due to surrounding elastic medium can be written as:

$$\Omega_i = \frac{1}{2}\int_0^L F_i\, w_i\, dx = \frac{1}{2}\int_0^L F_1\, w_1\, dx + \frac{1}{2}\int_0^L F_2\, w_2\, dx. \quad (15)$$

7. Hamilton's principle

Based on Hamilton's principle, the variational form of equations of motion can be written as [21]:

$$\delta \int_{t_1}^{t_2} \left[K_{pipes} + K_{fluid} - (U_i - \Omega_i) \right] dt = 0. \quad (16)$$

Nonlinear coupled differential equations are derived with rearranging the governing equations in terms of mechanical displacement (u, v and w) as well as electric potential (ϕ). For the sake of brevity, the relations are presented in Appendix A. In order to change the equations of motion in a dimensionless form, some parameters are defined in Table 1.

Table 1. Dimensionless parameters

Dimensionless parameters	Dimensional parameters
$\overline{u_i}, \overline{v_i}, \overline{w_i}$	$u_i, v_i, w_i / R_i$
$\zeta, \beta, \overline{h}, \overline{R_f}$	$x/L,\ R/L,\ h/L,\ R_f R/L^2$
$\eta, \overline{\phi}$	$\varphi e_{xxx}/GL, e_{x\theta\theta}/e_{xxx}$
$\tau, \overline{u_f}$	$\frac{t}{L}\sqrt{G/\rho_t}, \sqrt{\rho_f/G}\,u_f$
$\overline{\mu}, \overline{\rho}$	$\mu_e/L\sqrt{G\rho_f}, \rho_f/\rho_t$
$\overline{\psi_1}, \overline{\psi_2}, \overline{\psi_3}$	$\frac{e_{x\theta\theta}.\lambda_{xx}}{P_x.G}, \frac{e_{xxx}.\lambda_{xx}}{P_x.G}, \frac{\in_x.\lambda_{xx}}{P_x.e_{xxx}}$
$\overline{K_w}, \overline{K_G}, \overline{C_d}$	$\frac{K_w.R}{G}, \frac{K_G}{G.h}, \frac{C_d.R}{L\sqrt{G\rho_t}}$
C_1, C_2, C_3, C_4	$C_{x\theta x\theta}/G, C_{xx\theta\theta}/G, C_{\theta\theta\theta\theta}/G, C_{xxxx}/G$

It should be noted that identical geometric parameters are considered for both pipes in this study.

8. Solution method

Due to existence of nonlinear terms in equations of motion, they could not be solved analytically. Therefore numerical method must be employed to obtain frequency of coupled system. In this research, DQM is used to approximate the partial derivative of a function, with respect to a spatial variable at a specific discrete point, as a weighted linear sum of the function values at all discrete points chosen in the solution domain of the spatial variable. Let F be a function representing u_i, w_i, ψ_i and ϕ_i with respect to variables ξ and θ in the following domain of ($0 < \xi < L$, $0 < \theta < 2\pi$) having $N_\xi \times N_\theta$ grid points along these variables. The (n + m)th order partial derivative of $F(\xi,\theta)$ with respect to both ξ and θ can be considered at the point (ξ_i, θ_i) as [22]:

$$\frac{d^{n+m} F(\xi_i, \theta_j)}{d\xi^n d\theta^m} = \sum_{k=1}^{N_\xi} \sum_{l=1}^{N_\theta} A_{ik}^{(n)} B_{jl}^{(m)} F(\xi_k, \theta_l), \quad (17)$$

where $A_{ik}^{(n)}$ and $B_{jl}^{(m)}$ are the weighting coefficients associated with nth-order partial

derivative of $F(\xi,\theta)$ with respect to ξ at the discrete point ξ_i and m[th]-order derivative with respect to θ at θ_i, respectively [22]. Chebyshev polynomials [22] are selected for positions of the grid points. At first the solution of the equations of motion can be assumed as follows:

$$u(\zeta,\theta)=u(\zeta)e^{\omega\tau},\ v(\zeta,\theta)=v(\zeta)e^{\omega\tau},$$
$$w(\zeta,\theta)=w(\zeta)e^{\omega\tau},\ \phi(\zeta,\theta)=\phi(\zeta)e^{\omega\tau}. \quad (18)$$

in which, $\omega=\Omega h\sqrt{\frac{E}{\rho_f}}$ where ω is dimensionless natural frequency while Ω is the natural frequency.

According to DQM, boundary conditions for clamped-clamped shell can be written as [22]:

$$\begin{cases} w_{i1}=v_{i1}=u_{i1}=\phi_{i1}=0\Rightarrow & \sum_{j=1}^{N_\theta}A_{2j}w_{ji}=0, \\ w_{iN_\zeta}=v_{iN_\zeta}=u_{iN_\zeta}=\phi_{iN_\zeta}=0\Rightarrow & \sum_{j=1}^{N_\theta}A_{(N_\zeta-1)j}w_{ji}=0. \end{cases} \quad (19)$$

Imposing the above boundary conditions into equations of motion lead to the following constitutive matrix equation as:

$$M\ddot{Y}+\{C_{NL}+C_L\}\dot{Y}+\{K_{NL}+K_L\}Y=0, \quad (20)$$

where Y is the displacement vector, M is the mass matrix, $\{C_{NL}+C_L\}$ is the damping matrix and $\{K_{NL}+K_L\}$ is the stiffness matrix. Considering above boundary conditions, the matrix form of the equation (20) can be written as follows:

$$\begin{bmatrix}[K_{bb}] & [K_{bd}]\\ [K_{db}] & [K_{dd}]\end{bmatrix}\begin{Bmatrix}\{Y_b\}\\ \{Y_d\}\end{Bmatrix}+\begin{bmatrix}[0] & [0]\\ [C_{db}] & [C_{dd}]\end{bmatrix}\begin{Bmatrix}\{\dot{Y}_b\}\\ \{\dot{Y}_d\}\end{Bmatrix} \quad (21)$$
$$+\begin{bmatrix}[0] & [0]\\ [M_{db}] & [M_{dd}]\end{bmatrix}\begin{Bmatrix}\{\ddot{Y}_b\}\\ \{\ddot{Y}_d\}\end{Bmatrix}=0,$$

where *db* and *dd* represent boundary and domain points. As it was already said by assuming $\{\{Y_b\},\{Y_d\}\}=\{\bar{y}_b,\bar{y}_d\}e^{\omega\tau}$ the following standard eigenvalue problem yields:

$$AZ=\omega Z, \qquad Z=\{\{Y_b\},\{\dot{Y}_b\}\}^T, \quad (22)$$

where ω is the eigenvalues and matrix A can be defined as $A=\begin{bmatrix}0 & I\\ -M^{-1}K & -M^{-1}C\end{bmatrix}$, that I is unit matrix.

9. Numerical results and discussion

As mentioned in the previous sections, nonlinear frequency and critical fluid velocity for coupled composite pipes embedded in visco-Pasternak foundation was studied where PVDF and BNNT have been taken into account for smart matrix and piezoelectric fiber of the composite pipes, respectively. The structural properties of these materials are given in Table 2 [7, 23].

Table 2. Mechanical, electrical and thermal properties of PVDF and BNNTs

PVDF [23]	BNNT [7]
$S_{11}=S_{22}=S_{33}=385\times10^{-12}\,\mathrm{m^2/N}$	$C_{11}=C_{22}=C_{33}=2035GPa$
$S_{12}=S_{13}=S_{23}=-165\times10^{-12}\,\mathrm{m^2/N}$	$C_{12}=C_{23}=C_{13}=692GPa$
$S_{44}=S_{55}=S_{66}=1330\times10^{-12}\,\mathrm{m^2/N}$	$C_{44}=C_{55}=C_{66}=672GPa$
$d_{31}=20\times10^{-12}m/V$	$e_{33}=0.95C/m$
$d_{32}=3\times10^{-12}m/V$	$\in_{33}/\in_0=20$
$d_{33}=(-46\pm14)\times10^{-12}m/V$	$\in_0=8.854185\times10^{-12}(F/m)$
$d_{24}=d_{15}=0$	

In addition, the geometrical properties of composite pipes and the constants of elastic medium are given follows:

$$r=1m,\ h=0.05m,\ \rho_f=800\frac{Kg}{m^3},\ l/r=15,$$
$$\overline{K}_W=100,\overline{K}_G=0.1,\overline{C}_d=0.01. \quad (23)$$

Figures 2a and 2b illustrate the effect of orientation angle on vibration of coupled system. Since the orientation angle of fiber can be affected the feature of materials, it is a very important factor. This coupled system has been reinforced by BNNTs that can be aligned in different direction. It is obvious from Figures 2a that increasing angle cause to decrease the frequency and critical fluid velocity. Also, the stiffness of coupled system increases when the

fibers are arranged along the axis of oil pipes. Therefore, $\alpha = 0$ is the best fiber angle to obtain more stability.

Figures 3a and 3b show the effect of volume fraction of BNNT in composite oil pipes on vibration of coupled system. It is found that the strength of composite pipes increase significantly by increasing the volume fraction of BNNT, and consequently the stability of coupled system enhances. Designer could meet their purposes to manufacturing the resistant structures by selecting the suitable percent of fiber.

Figures 4a and 4b illustrate the effect of different elastic medium on dimensionless frequency versus dimensionless fluid velocity. It is obvious that existence of Winkler and Pasternak foundation enlarge the stability region of coupled system and increase the frequency too. It is worth to note that in the presence of damping the positive effect of the elastic medium reduces in both cases including Winkler and Pasternak types. It is seen that $\mathrm{Im}(\omega)$ increases by increasing the elastic foundation stiffness and decrease as u_f increases. It is clear that the elastic foundation increases the stability of coupled system.

Figure 5a and 5b depict the effect of temperature changes on imaginary and real part of coupled system frequencies. It is evident from these figures that increasing temperature change causes to decrease critical fluid velocity. Therefore, minimum temperature change should be selected in such coupled system.

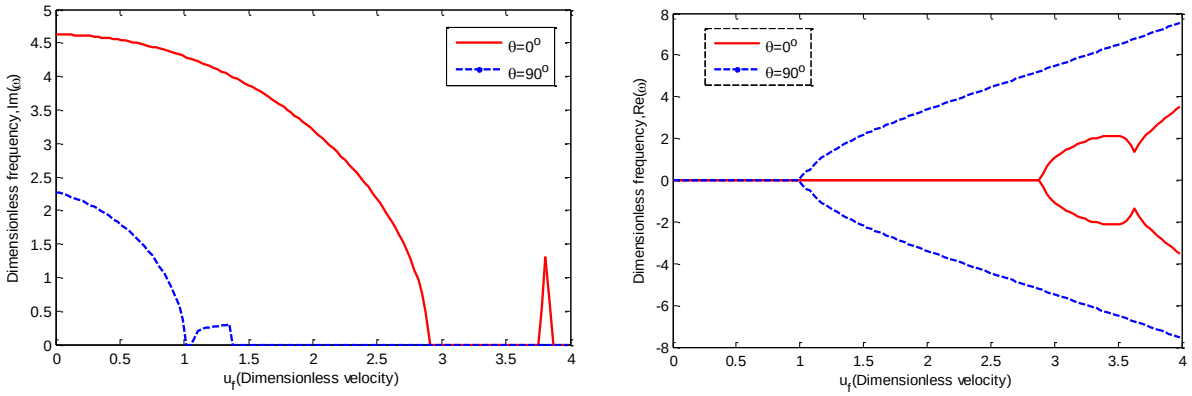

(a) **(b)**

Fig. 2. Effect of angle orientation of BNNTS on dimensionless natural and damping frequencies

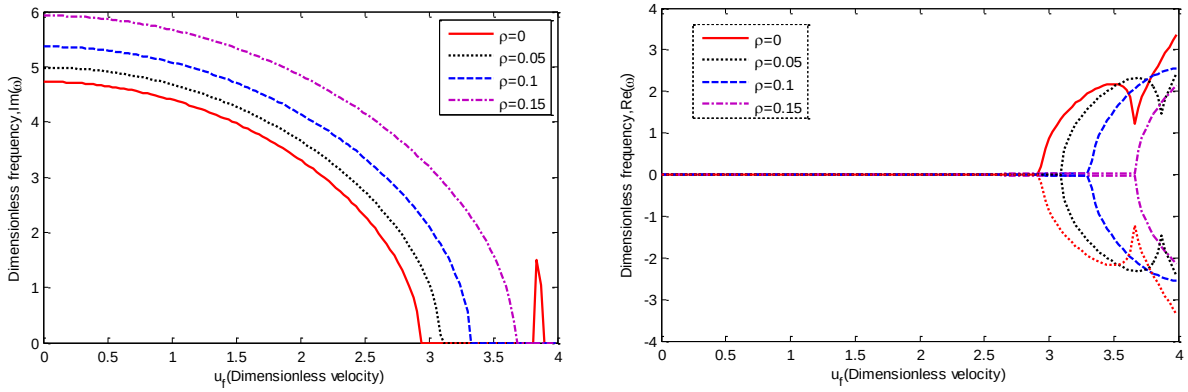

(a) **(b)**

Fig. 3. Dimensionless natural and damping frequencies versus dimensionless fluid velocity for various volume fractions of BNNTs

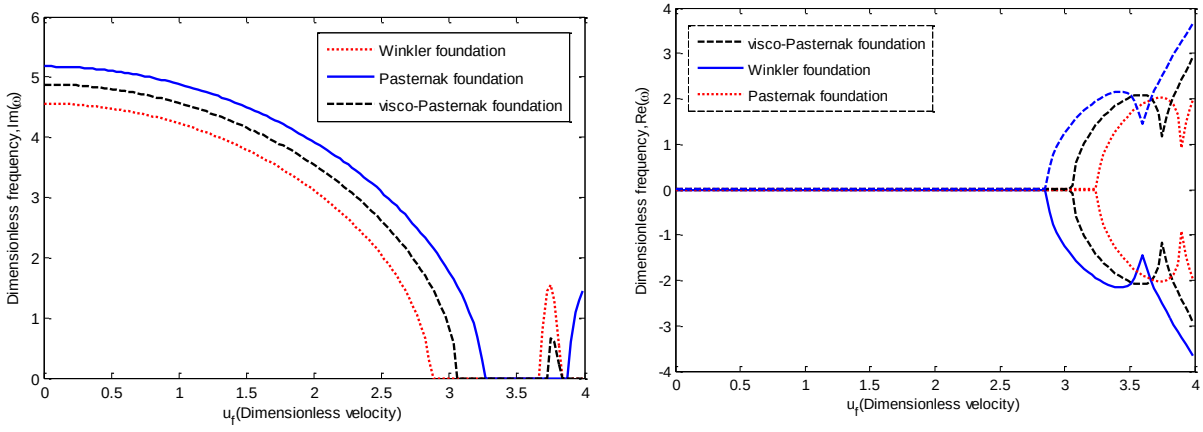

(a) **(b)**

Fig. 4. Effect of elastic medium on stability of coupled BNNTRC oil pipes

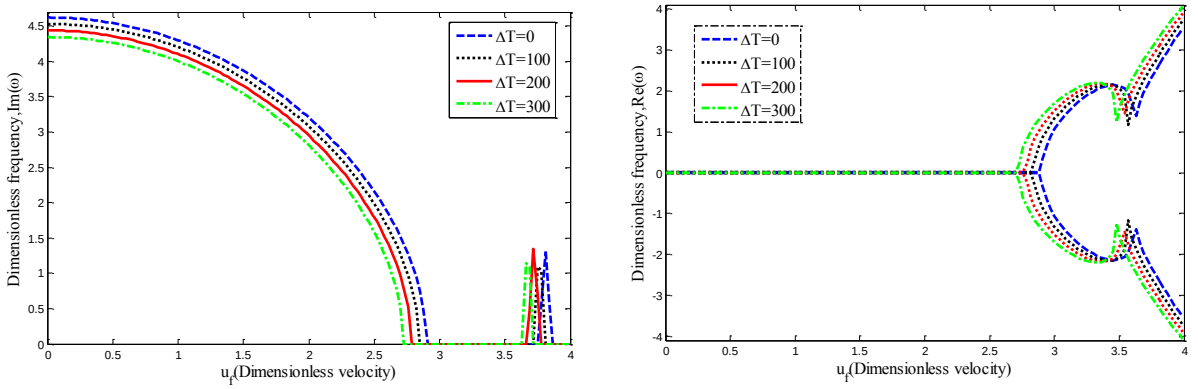

(a) **(b)**

Fig. 5. Effect of Temperature changes on imaginary and real part of frequencies of coupled BNNTRC oil pipes

Figure 6 demonstrates the effects of density of fluid on the nonlinear vibration of coupled system. Two kind of oil with different Iso grades have been selected to study the effect of density of fluid. Results show that the density of fluid is an important parameter that affects the results. So that by increasing the density, both frequency and critical velocity increase.

Figure 7 illustrates the dimensionless transverse displacement of two composite tubes along the longitudinal axis. This figure shows both in phase (synchronous) and out of phase (asynchronous) vibrations. In addition, clamped-clamped boundary conditions at the both ends of composite tubes are satisfied. As can be seen, in the synchronous vibration both tubes are moved together, while the motion of upper and lower tubes is opposite in asynchronous case.

Figure 8 depicts distribution of electric potential (ϕ) in the coupled system for various u_f . As can be seen, constant electrical boundary conditions at the both ends of composite tubes are satisfied. In Figure 8, electric potential, ϕ , is directly related to u_f . Due to coupling between mechanical and electrical fields in piezoelectric materials, stress and deformation of tubes lead to higher electric potential as fluid velocity increases. It can be used in the warning system and sensors.

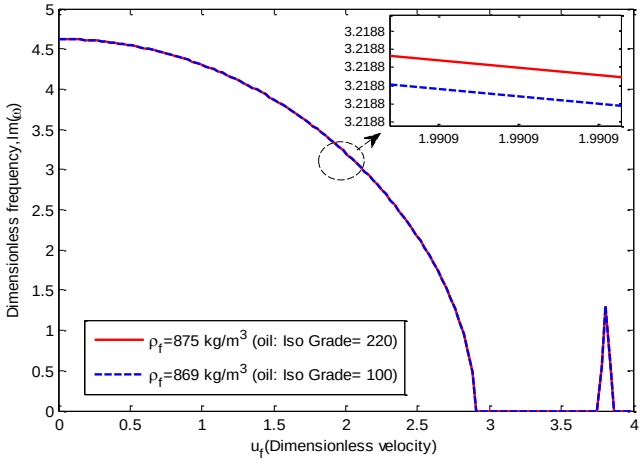

Fig. 6. Effect of density of oil conveyed in composite oil pipes on dimensionless natural frequency

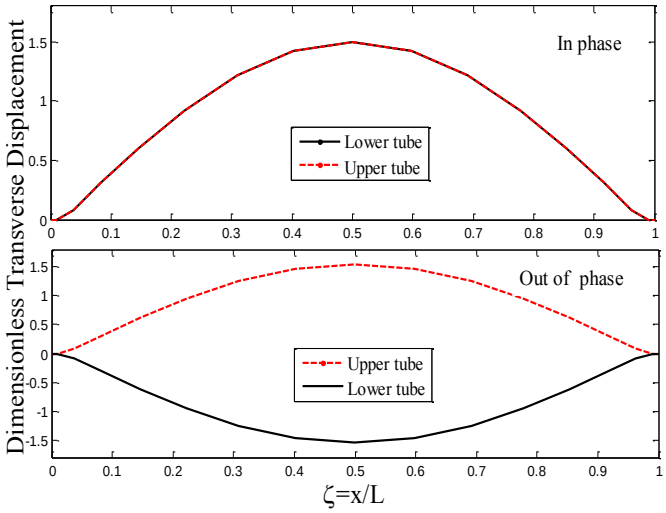

Fig. 7. Dimensionless transverse displacement of two composite tubes along the longitudinal axis

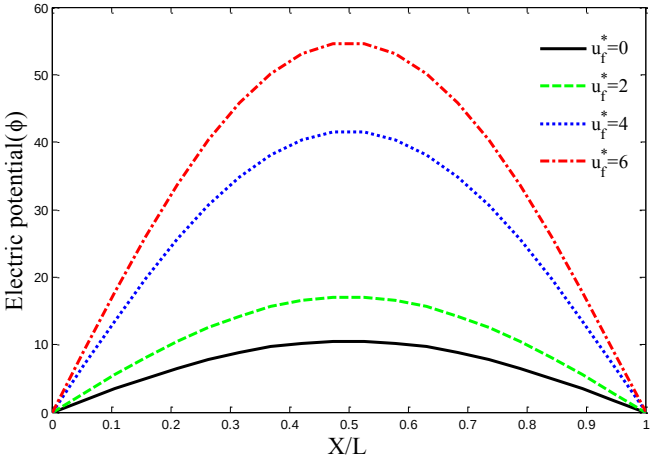

Fig. 8. Distribution of electric potential (ϕ) in the coupled system for various u_f

Conclusion

In this study, nonlinear vibration and stability of a smart coupled composite oil pipes reinforced by BNNTs conveying viscose fluid embedded in a visco-Pasternak foundation was considered. The composite consist of fibers and matrix, PVDF was used as a matrix and BNNTs as smart nano-fibers in longitudinal direction. The governing equations of motion were obtained using Hamilton principle. The nonlinear frequency and critical fluid velocity were the result of solving equations of motion with clamped–clamped boundary conditions using DQ method. The results showed that angle and volume percent of fibers can affect the system stability, also, the material of matrix and fibers change the mechanical behaviour of coupled system, in this regard, piezo-electrics can be utilized as smart fibers in composite structure. Also, it can be seen that the trend of figures have good agreement with the previous researches. Results of this investigation can be used in oil refineries.

Acknowledgments

The author would like to thank the reviewers for their comments and suggestions to improve the clarity of this article. The authors are grateful to University of Kashan for supporting this work by Grant No. 363443/38. They would also like to thank the Iranian Nanotechnology Development Committee for their financial support.

Appendix A

Governing equations of motion:

δu_1 :

$$-2\pi h_1 C_{xx\theta\theta}\frac{dw_1}{dx}-2\pi h_1 C_{xx\theta\theta}\frac{d^2v_1}{d\theta dx}-2\pi h_1\frac{C_{x\theta x\theta}}{R_1}\frac{d^2u_1}{d\theta^2}-2\pi h_1 C_{x\theta x\theta}\frac{d^2v_1}{d\theta dx}+\pi R_1 h_1\lambda_{xx}\frac{dT}{dx}$$
$$-2\pi R_1 h_1 e_{xxx}\frac{d^2\phi_1}{dx^2}-2\pi h_1\frac{C_{x\theta x\theta}}{R_1}\frac{dw_1}{dx}\frac{d^2w_1}{d\theta^2}-2\pi h_1\frac{C_{x\theta x\theta}}{R_1}\frac{dw_1}{d\theta}\frac{d^2w_1}{d\theta dx}-2\pi h_1\frac{C_{xx\theta\theta}}{R_1}\frac{dw_1}{d\theta}\frac{d^2w_1}{d\theta dx} \quad (A.1)$$
$$-2\pi R_1 h_1 C_{xxxx}\frac{dw_1}{dx}\frac{d^2w_1}{dx^2}-mf\ Uf^2\frac{d^2w_1}{dx^2}\frac{dw_1}{dx}+m_1\frac{d^2u_1}{dt^2}+mf\frac{d^2u_1}{dt^2}-mf\ KnUf\frac{dw_1}{dx}\frac{d^2w_1}{dtdx}=0$$

δu_2 :

$$-2\pi h_2\frac{C_{x\theta x\theta}}{R_2}\frac{d^2u_2}{d\theta^2}-2\pi h_2 C_{xx\theta\theta}\frac{d^2v_2}{d\theta dx}-2\pi h_2 C_{x\theta x\theta}\frac{d^2v_2}{d\theta dx}-2\pi h_2 C_{xx\theta\theta}\frac{dw_2}{dx}-2\pi h_2\frac{C_{x\theta x\theta}}{R_2}\frac{d^2w_2}{d\theta^2}\frac{dw_2}{dx}$$
$$-2\pi h_2\frac{C_{x\theta x\theta}}{R_2}\frac{dw_2}{d\theta}\frac{d^2w_2}{d\theta dx}-2\pi h_2\frac{C_{xx\theta\theta}}{R_2}\frac{dw_2}{d\theta}\frac{d^2w_2}{d\theta dx}+\pi R_2 h_2\lambda_{xx}\frac{dT}{dx}-2\pi R_2 h_2 e_{xxx}\frac{d^2\phi_2}{dx^2} \quad (A.2)$$
$$-2\pi R_2 h_2 C_{xxxx}\frac{dw_2}{dx}\frac{d^2w_2}{dx^2}+mf\frac{d^2u_2}{dt^2}-mf\ Uf^2\frac{d^2w_2}{dx^2}\frac{dw_2}{dx}+m_2\frac{d^2u_2}{dt^2}-mf\ XKnUf\frac{dw_2}{dx}\frac{d^2w_2}{dtdx}=0$$

δv_1 :

$$-2\pi R_1 h_1 C_{x\theta x\theta}\frac{d^2v_1}{dx^2}-2\pi h_1 C_{x\theta x\theta}\frac{dw_1}{dx}\frac{d^2w_1}{d\theta dx}-2\pi h_1 C_{x\theta x\theta}\frac{dw_1}{d\theta}\frac{d^2w_1}{dx^2}-2\pi h_1 C_{xx\theta\theta}\frac{dw_1}{dx}\frac{d^2w_1}{d\theta dx}$$
$$-2\pi h_1\frac{C_{\theta\theta\theta\theta}}{R_1^2}\frac{dw_1}{d\theta}\frac{d^2w_1}{d\theta^2}-2\pi h_1 C_{xx\theta\theta}\frac{d^2u_1}{d\theta dx}-2\pi h_1\frac{C_{\theta\theta\theta\theta}}{R_1}\frac{dw_1}{d\theta}-2\pi h_1 C_{x\theta x\theta}\frac{d^2u_1}{d\theta dx}+m_1\frac{d^2v_1}{dt^2}+mf\frac{d^2v_1}{dt^2}=0 \quad (A.3)$$

δv_2 :

$$-2\pi R_2 h_2 C_{x\theta x\theta}\frac{d^2v_2}{dx^2}-2\pi h_2\frac{C_{\theta\theta\theta\theta}}{R_2}\frac{dw_2}{d\theta}-2\pi h_2 C_{x\theta x\theta}\frac{d^2u_2}{d\theta dx}-2\pi h_2 C_{xx\theta\theta}\frac{d^2u_2}{d\theta dx}-2\pi h_2 C_{x\theta x\theta}\frac{dw_2}{dx}\frac{d^2w_2}{d\theta dx}$$
$$-2\pi h_2 C_{x\theta x\theta}\frac{dw_2}{d\theta}\frac{d^2w_2}{dx^2}-2\pi h_2 C_{xx\theta\theta}\frac{dw_2}{dx}\frac{d^2w_2}{d\theta dx}-2\pi h_2\frac{C_{\theta\theta\theta\theta}}{R_2^2}\frac{dw_2}{d\theta}\frac{d^2w_2}{d\theta^2}+mf\frac{d^2v_2}{dt^2}+m_2\frac{d^2v_2}{dt^2}=0 \quad (A.4)$$

$\delta\phi_1$:

$$2\pi R_1 h_1 \epsilon_x \frac{d^2\phi_1}{dx^2} - 2\frac{\pi h_1 e_{x\theta\theta}}{R_1}\frac{dw_1}{d\theta}\frac{d^2w_1}{d\theta dx} - 2\pi h_1 e_{x\theta\theta}\frac{d^2v_1}{d\theta dx} - 2\pi R_1 h_1 e_{xxx}\frac{dw_1}{dx}\frac{d^2w_1}{dx^2}$$
$$-2\pi h_1 e_{x\theta\theta}\frac{dw_1}{dx} + \pi R_1 h_1 p_x \frac{dT}{dx} - 2\pi R_1 h_1 e_{xxx}\frac{d^2u_1}{dx^2} = 0 \tag{A.5}$$

$\delta\phi_2$:

$$2\pi R_2 h_2 \epsilon_x \frac{d^2\phi_2}{dx^2} - 2\frac{\pi h_2 e_{x\theta\theta}}{R_2}\frac{dw_2}{d\theta}\frac{d^2w_2}{d\theta dx} - 2\pi h_2 e_{x\theta\theta}\frac{d^2v_2}{d\theta dx} - 2\pi h_2 e_{x\theta\theta}\frac{dw_2}{dx}$$
$$-2\pi R_2 h_2 e_{xxx}\frac{dw_2}{dx}\frac{d^2w_2}{dx^2} + \pi R_2 h_2 p_x \frac{dT}{dx} - 2\pi R_2 h_2 e_{xxx}\frac{d^2u_2}{dx^2} = 0 \tag{A.6}$$

δw_1 :

$$2mf\ KnUf\frac{d^2w_1}{dtdx} - 2\pi h_1\frac{C_{xx\theta\theta}}{R_1}\frac{du_1}{dx}\frac{d^2w_1}{d\theta^2} - 2\pi R_1 h_1 C_{xxxx}\frac{d^2w_1}{dx^2}\frac{du_1}{dx} - 2\pi R_1 h_1 C_{xxxx}\frac{dw_1}{dx}\frac{d^2u_1}{dx^2}$$
$$-2\frac{\pi h_1 C_{x\theta x\theta}}{R_1}\left(\frac{dw_1}{d\theta}\right)^2\frac{d^2w_1}{dx^2} - 2\frac{\pi h_1 C_{x\theta x\theta}}{R_1}\left(\frac{dw_1}{dx}\right)^2\frac{d^2w_1}{d\theta^2} - 3\frac{\pi h_1 C_{\theta\theta\theta\theta}}{R_1^3}\left(\frac{dw_1}{d\theta}\right)^2\frac{d^2w_1}{d\theta^2}$$
$$-\frac{\pi h_1 C_{xx\theta\theta}}{R_1}\left(\frac{dw_1}{d\theta}\right)^2\frac{dw_1^2}{dx^2} - \frac{\pi h_1 C_{xx\theta\theta}}{R_1}\left(\frac{dw_1}{dx}\right)^2\frac{d^2w_1}{d\theta^2} - mf\ KnUf\frac{dw_1}{dx}\frac{dw_1}{dt}\frac{d^2w_1}{dx^2}$$
$$-4\frac{\pi h_1 C_{x\theta x\theta}}{R_1}\frac{d^2w_1}{d\theta dx}\frac{du_1}{d\theta} - 2\frac{\pi h_1 C_{x\theta x\theta}}{R_1}\frac{d^2u_1}{d\theta^2}\frac{dw_1}{dx} - 2\frac{\pi h_1 C_{x\theta x\theta}}{R_1}\frac{dw_1}{d\theta}\frac{d^2u_1}{d\theta dx} - 2\frac{\pi h_1 C_{\theta\theta\theta\theta}}{R_1^2}w_1\frac{d^2w_1}{d\theta^2}$$
$$+2\frac{\pi h_1 C_{\theta\theta\theta\theta}}{R_1}\frac{dv_1}{d\theta} - \frac{\pi h_1 C_{\theta\theta\theta\theta}}{R_1^2}\left(\frac{dw_1}{d\theta}\right)^2 + 2\frac{\pi h_1 C_{\theta\theta\theta\theta}w_1}{R_1} - 2\frac{\pi h_1 C_{xx\theta\theta}}{R_1}\frac{dw_1}{d\theta}\frac{d^2u_1}{d\theta dx} - 2\frac{\pi h_1 e_{x\theta\theta}}{R_1}\frac{d^2w_1}{d\theta^2}\frac{d\phi_1}{dx}$$
$$+\frac{\pi h_1\lambda_{\theta\theta}T}{R_1}\frac{d^2w_1}{d\theta^2} - 2\pi R_1 h_1 e_{xxx}\frac{d\phi_1}{dx}\frac{d^2w_1}{dx^2} - 2\pi R_1 h_1 e_{xxx}\frac{dw_1}{dx}\frac{d^2\phi_1}{dx^2} + \pi R_1 h_1\lambda_{xx}T\frac{d^2w_1}{dx^2}$$
$$-2\frac{\pi h_1 C_{\theta\theta\theta\theta}}{R_1^2}\frac{dw_1}{d\theta}\frac{d^2v_1}{d\theta^2} - 2\frac{\pi h_1 C_{\theta\theta\theta\theta}}{R_1^2}\frac{d^2w_1}{d\theta^2}\frac{dv_1}{d\theta} + 2\pi h_1 C_{xx\theta\theta}\frac{du_1}{dx} - \pi h_1 C_{xx\theta\theta}\left(\frac{dw_1}{dx}\right)^2$$
$$+2\pi h_1 e_{x\theta\theta}\frac{d\phi}{dx}_1 - \pi h_1\lambda_{\theta\theta}T + \pi h_1\lambda_{x\theta}\frac{dT}{dx}\frac{dw_1}{d\theta} + m_1\frac{dw_1^2}{dt^2} - I_1\frac{d^4w_1}{dt^2dx^2} - I_{f1}\frac{d^4w_1}{dt^2dx^2}$$
$$+mf\frac{d^2w_1}{dt^2} - 2KG\frac{d^2w_1}{dx^2} + KG\frac{d^2w_2}{dx^2} - 4\frac{\pi h_1 C_{xx\theta\theta}}{R_1}\frac{dw_1}{d\theta}\frac{dw_1}{dx}\frac{d^2w_1}{d\theta dx}$$
$$-8\frac{\pi h_1 C_{x\theta x\theta}}{R_1}\frac{dw_1}{d\theta}\frac{dw_1}{dx}\frac{d^2w_1}{d\theta dx} + \frac{1}{12}\pi R_1 h_1^3 C_{xxxx}\frac{d^4w_1}{dx^4} + \frac{1}{6}\frac{\pi h_1^3 C_{xx\theta\theta}}{R_1}\frac{d^4w_1}{d\theta^2dx^2} + \frac{1}{12}\frac{\pi h_1^3 C_{\theta\theta\theta\theta}}{R_1^3}\frac{d^4w_1}{d\theta^4}$$
$$+\frac{1}{3}\frac{\pi h_1^3 C_{x\theta x\theta}}{R_1}\frac{d^4w_1}{d\theta^2dx^2} + 2\pi h_1\lambda_{x\theta}T\frac{d^2w_1}{d\theta dx} - mf\ KnUf\frac{d^2u_1}{dtdx}\frac{dw_1}{dx} - mf\ KnUf\frac{d^2w_1}{dx^2}\frac{du_1}{dt}$$
$$-2\pi h_1 C_{x\theta x\theta}\frac{dw_1}{dx}\frac{d^2v_1}{d\theta dx} - 4\pi h_1 C_{x\theta x\theta}\frac{dv_1}{dx}\frac{d^2w_1}{d\theta dx} - 2\pi h_1 C_{x\theta x\theta}\frac{d^2v_1}{dx^2}\frac{dw_1}{d\theta} - 2\pi h_1 C_{xx\theta\theta}\frac{d^2w_1}{dx^2}\frac{dv_1}{d\theta}$$
$$-2\pi h_1 C_{xx\theta\theta}\frac{dw_1}{dx}\frac{d^2v_1}{d\theta dx} - 2\pi h_1 C_{xx\theta\theta}w_1\frac{d^2w_1}{dx^2} + mf\ Uf^2\frac{d^2w_1}{dx^2} - \frac{I_{f1}}{R_1^2}\frac{d^4w_1}{dt^2d\theta^2} - \frac{I_1}{R_1^2}\frac{d^4w_1}{dt^2d\theta^2}$$
$$+2C_d\frac{dw_1}{dt} + 2KW w_1 - KW w_2 - C_d\frac{dw_2}{dt} = 0 \tag{A.7}$$

δw_2 :

$$
\begin{aligned}
&-8\frac{\pi h_2 C_{x\theta x\theta}}{R_2}\frac{d^2w_2}{d\theta dx}\frac{dw_2}{dx}\frac{dw_2}{d\theta}-4\frac{\pi h_2 C_{xx\theta\theta}}{R_2}\frac{dw_2}{d\theta}\frac{dw_2}{dx}\frac{d^2w_2}{d\theta dx}-\pi h_2\lambda_{\theta\theta}T+2\pi h_2 e_{x\theta\theta}\frac{d\phi_2}{dx}\\
&-\frac{\pi R_2 h_2 C_{xx\theta\theta}}{R}\left(\frac{dw_2}{dx}\right)^2-\frac{\pi R_2 h_2 C_{\theta\theta\theta\theta}}{R^3}\left(\frac{dw_2}{d\theta}\right)^2+2\pi h_2 C_{xx\theta\theta}\frac{du_2}{dx}+2\frac{\pi h_2 C_{\theta\theta\theta\theta}}{R_2}\frac{dv_2}{d\theta}\\
&-2\frac{\pi h_2 C_{\theta\theta\theta\theta}}{R_2^2}\frac{dv_2}{d\theta}\frac{d^2w_2}{d\theta^2}+2\frac{\pi h_2 C_{\theta\theta\theta\theta}}{R_2}w_2-2\pi h_2 C_{xx\theta\theta}\frac{d^2w_2}{dx^2}\frac{dv_2}{d\theta}-2\pi h_2 C_{xx\theta\theta}\frac{dw_2}{dx}\frac{d^2v_2}{d\theta dx}\\
&-2\pi h_2 C_{xx\theta\theta}w_2\frac{d^2w_2}{dx^2}-2\frac{\pi h_2 C_{x\theta x\theta}}{R_2}\left(\frac{dw_2}{d\theta}\right)^2\frac{d^2w_2}{dx^2}-2\frac{\pi h_2 C_{x\theta x\theta}}{R_2}\left(\frac{dw_2}{dx}\right)^2\frac{d^2w_2}{d\theta^2}\\
&-3\frac{\pi h_2 C_{\theta\theta\theta\theta}}{R_2^3}\left(\frac{dw_2}{d\theta}\right)^2\frac{d^2w_2}{d\theta^2}-\frac{\pi h_2 C_{xx\theta\theta}}{R_2}\frac{d^2w_2}{dx^2}\left(\frac{dw_2}{d\theta}\right)^2-\frac{\pi h_2 C_{xx\theta\theta}}{R_2}\left(\frac{dw_2}{dx}\right)^2\frac{d^2w_2}{d\theta^2}\\
&-2\frac{\pi h_2 C_{xx\theta\theta}}{R_2}\frac{d^2w_2}{d\theta^2}\frac{du_2}{dx}-4\frac{\pi h_2 C_{x\theta x\theta}}{R_2}\frac{d^2w_2}{d\theta dx}\frac{du_2}{d\theta}-2\frac{\pi h_2 C_{x\theta x\theta}}{R_2}\left(\frac{d^2u_2}{d\theta^2}\right)\frac{dw_2}{dx}\\
&-2\frac{\pi h_2 C_{x\theta x\theta}}{R_2}\frac{d^2u_2}{d\theta dx}\frac{dw_2}{d\theta}-mf\ KnXUf\frac{dw_2}{dt}\frac{dw_2}{dx}\frac{d^2w_2}{dx^2}-2\frac{\pi h_2 e_{x\theta\theta}}{R_2}\frac{d\phi_2}{dx}\frac{d^2w_2}{d\theta^2}\\
&-2\frac{\pi h_2 C_{\theta\theta\theta\theta}}{R_2^2}w_2\frac{d^2w_2}{d\theta^2}-2\frac{\pi h_2 C_{xx\theta\theta}}{R_2}\frac{d^2u_2}{d\theta dx}\frac{dw_2}{d\theta}-2\pi h_2 C_{x\theta x\theta}\frac{dw_2}{dx}\frac{d^2v_2}{d\theta dx}\\
&-4\pi h_2 C_{x\theta x\theta}\frac{dv_2}{dx}\frac{d^2w_2}{d\theta dx}-2\pi h_2 C_{x\theta x\theta}\frac{dw_2}{d\theta}\frac{d^2v_2}{dx^2}-2\frac{\pi h_2 C_{\theta\theta\theta\theta}}{R_2^2}\frac{d^2v_2}{d\theta^2}\frac{dw_2}{d\theta}\\
&+2\pi h_2\lambda_{x\theta}T\frac{d^2w_2}{d\theta dx}+\frac{\pi R_2 h_2\lambda_{\theta\theta}T}{R^2}\frac{d^2w_2}{d\theta^2}+\pi R_2 h_2\lambda_{xx}T\frac{d^2w_2}{dx^2}+\frac{1}{12}\frac{\pi h_2^3 C_{\theta\theta\theta\theta}}{R_2^3}\frac{d^4w_2}{d\theta^4}\\
&+\frac{1}{3}\frac{\pi h_2^3 C_{x\theta x\theta}}{R_2}\frac{d^4w_2}{d\theta^2dx^2}+\frac{1}{6}\frac{\pi h_2^3 C_{xx\theta\theta}}{R_2}\frac{d^4w_2}{d\theta^2dx^2}-2\pi R_2 h_2 C_{xxxx}\frac{d^2w_2}{dx^2}\frac{du_2}{dx}\\
&-2\pi R_2 h_2 C_{xxxx}\frac{dw_2}{dx}\frac{d^2u_2}{dx^2}-mf\ KnXUf\frac{d^2u_2}{dtdx}\frac{dw_2}{dx}-mf\ KnXUf\frac{du_2}{dt}\frac{d^2w_2}{dx^2}+m_2\frac{d^2w_2}{dt^2}\\
&-2\pi R_2 h_2 e_{xxx}\frac{d^2w_2}{dx^2}\frac{d\phi_2}{dx}-2\pi R_2 h_2 e_{xxx}\frac{dw_2}{dx}\frac{d^2\phi_2}{dx^2}+KG\frac{d^2w_1}{dx^2}-2KG\frac{d^2w_2}{dx^2}-I_{f2}\frac{d^4w_2}{dt^2dx^2}\\
&+mf\frac{d^2w_2}{dt^2}-\frac{I_{f2}}{R_2^2}\frac{d^4w_2}{dt^2d\theta^2}+mf\ Uf^2\frac{d^2w_2}{dx^2}-\frac{I_2}{R_2^2}\frac{d^4w_2}{dt^2d\theta^2}-I_2\frac{d^4w_2}{dt^2dx^2}+2mf\ KnXUf\frac{d^2w_2}{dtdx}\\
&-C_d\frac{dw_1}{dt}-KW\,w_1+\frac{1}{12}\pi R_2 h_2^3 C_{xxxx}\frac{d^4w_2}{dx^4}+\pi h_2\lambda_{x\theta}\frac{dT}{dx}\frac{dw_2}{d\theta}+2KW\,w_2+2C_d\frac{dw_2}{dt}=0
\end{aligned}
\tag{A.8}
$$

References

[1]. Shu, C. (1996). "Free vibration analysis of composite laminated conical shells by generalized differential quadrature." J. Sound. Vib., vol. 194, PP. 587-604.

[2]. Kadoli, R. and Ganesan, N. (2003). "Free vibration and buckling analysis of composite cylindrical shells conveying hot fluid." Compos. Struct., vol. 60 , PP. 19–32.

[3]. Wang, X. and Zhong, Z. (2003). "Three-dimensional solution of smart laminated anisotropic circular cylindrical shells with imperfect bonding." Int. J. Solids. Struct., vol. 40 PP. 5901–5921.

[4]. Salehi-Khojin, A. and Jalili, N. (2008). "Buckling of boron nitride nano-tube reinforced piezoelectric polymeric composites subject to combined electro-thermo-mechanical loadings." Compos. Sci. Technol., vol. 68, PP. 1489-1501.

[5]. Amabili, M., Karagiozis, K. and Paidoussis, M.P. (2009). "Effect of geometric imperfections on non-linear stability of circular cylindrical shells conveying fluid." Int. J. Solids. Struct., vol. 44 , PP. 276–289.

[6]. Rahmani, O., Khalili, S.M.R. and Malekzadeh, K. (2009). "Free vibration response of composite sandwich cylindrical shell with

flexible core." Compos. Struct., vol. 92, PP. 1269–1281.

[7]. Zhou, X. and Wang, L. (2012). "Vibration and stability of micro-scale cylindrical shells conveying fluid based on modified couple stress theory." Micro Nano Lett., vol. 7, PP. 679–684.

[8]. Ghorbanpour Arani, A., Amir, S., Shajari, A.R. and Mozdianfard, M.R. (2012). "Electro-thermo-mechanical buckling of DWBNNTs embedded in bundle of CNTs using nonlocal piezoelasticity cylindrical shell theory." Compos. Part B: Engineering., vol. 43, PP. 195-203.

[9]. Ghorbanpour Arani, A., Shokravi, M., Amir, S. and Mozdianfard, M.R. (2012). "Nonlocal electro-thermal transverse vibration of embedded fluid-conveying DWBNNTs." J. Mech. Sci. Technol., vol. 26 , PP. 1455-1462.

[10]. Ghorbanpour Arani, A., Shajari, A.R., Amir, S. and Loghman, A. (2012). "Electro-thermo-mechanical nonlinear nonlocal vibration and instability of embedded micro-tube reinforced by BNNT, conveying fluid." Physica E., vol. 45, PP. 109–121.

[11]. Ghorbanpour Arani, A., Abdollahian, M., Kolahchi, R. (2014). "Nonlinear Vibration of Embedded Smart Composite Microtube Conveying Fluid Based on Modified Couple Stress Theory." Polym. Compos. , PP. 1-11.

[12]. Tan, P. and Tong, L. (2001). "Micro-electro-mechanics models for piezoelectric-fiber reinforced composite materials." Compos. Sci. Technol., vol. 61, PP. 759–769.

[13]. Tan, P. and Tong, L. (2001). "Micromechanics models for non-linear behavior of piezoelectric fiber reinforced composite materials." Int. J. Solids. Struct., vol. 38, PP. 8999–9032.

[14]. Mase, G.T. and Mase, G.E. (1999). Continuum Mechanics for Engineers. Second ed., CRC Press, Michigan.

[15]. Ghorbanpour Arani, A., Kolahchi, R. and Khoddami Maraghi, Z. (2013). "Nonlinear vibration and instability of embedded double-walled boron nitride nano-tubes based on nonlocal cylindrical shell theory." APPl. Math. Modell., vol. 37 , PP. 7685–7707.

[16]. Zhou, X. and Wang, L. (2012). "vibration and stability of micro-scale cylindrical shells conveying fluid based on modified couple stress theory." Micro. Nano. Lett., vol. 7, PP. 679–684.

[17]. Fox, W.P., Pritchard, J. and McDonald, A.T. (2005). Introduction to Fluid Mechanics. sixth ed., John Wiley & Sons Pub, New York.

[18]. Karniadakis, G., Beskok, A. and Aluru, N. (2005). Micro-flows Nano-flows: Fundamental simulation. Springer Pub, New York.

[19]. Mirramezani, M. and Mirdamadi, H.R. (2012). "The effects of Knudsen-dependent flow velocity on vibrations of a nano-pipe conveying fluid." Arch. APPl. Mech., vol. 82, PP. 879-890.

[20]. Kaviani, F. and Mirdamadi, H.R. (2012). "Influence of Knudsen number on fluid viscosity for analysis of divergence in fluid conveying nano-tubes." Comput. Mater. Sci., vol. 61, PP. 270–277.

[21]. Ghorbanpour Arani, A. and Amir, S. (2013). "Electro-thermal vibration of visco-elastically coupled BNNT systems conveying fluid embedded on elastic foundation via strain gradient theory." Physica B., vol. 419, PP.1–6.

[22]. Shu, C. (2000). Differential Quadrature and its APPlication in Engineering. Springer Pub, London.

[23]. Liu, Z.H., Pan, C.T., Lin, L.W. and Lai, H.W. (2013). "Piezoelectric properties of PVDF/MWCNT nano-fiber using near-field electrospinning." Sens. Actuators, vol. 193, PP. 13– 24.